CLS
COLLECTE LOCALISATION SATELLITES

Consortium Members

TU Delft Delft University of Technology | SATOC Satellite Oceanographic Consultants | DTU Space National Space Institute | isardSAT | National Oceanography Centre Natural Environment Research Council | NOVELTIS | Starlab Living Science | U.PORTO Faculdade de Ciências Universidade do Porto

ESA Cryosat Plus for Oceans

Validation Report: WP5000 Assessment of CPP SAR Retracking

Reference:	CLS-DOS-NT-14-113
Nomenclature:	CP4O-WP5000-VR-06
Issue:	1. 0
Date:	Jun. 20, 14

esa European Space Agency

cnes CENTRE NATIONAL D'ÉTUDES SPATIALES

Chronology Issues:			
Issue:	Date:	Reason for change:	Author
1.0	20/06/14	Creation of Issue 1.0 document	S. Labroue M. Raynal T. Moreau

People involved in this issue:		
Written by (*):	S. Labroue, M. Raynal, T. Moreau (CLS)	Date + Initials:(visa or ref)
Checked by (*):	S. Labroue (CLS)	Date + Initial:(visa ou ref)
Approved by (*):	F. Boy (CNES)	Date + Initial:(visa ou ref)
Application authorized by (*):	ESA N. Picot (CNES)	Date + Initial:(visa ou ref)

**In the opposite box: Last and First name of the person + company if different from CLS*

Index Sheet:	
Context:	
Keywords:	[Mots clés]
Hyperlink:	

Distribution:		
Company	Means of distribution	Names
CLS	Notification	

List of tables and figures

List of figures:

Figure 1: SWH map in July 2012. 2

Figure 2: SWH map in January 2013 3

Figure 3: PSD of SAR and LRM SLA 5

Figure 4: PSD of SAR and LRM SWH 6

Figure 5: PSD of SAR and LRM Sigma0 6

Figure 6: SLA differences (upper panel) and PLRM SWH (bottom panel) for ascending passes 9

Figure 7: SLA differences (upper panel) and PLRM SWH (bottom panel) for descending passes . 10

Figure 8 – Range difference binned per PLRM SWH for ascending (red) and descending (blue) passes 11

Figure 9 – SAR – PLRM Range difference (m) binned per PLRM SWH and Roll Angle for ascending passes (mean on the left and density on the right) 13

Figure 10 – SAR – PLRM Range difference (m) binned per PLRM SWH and Roll Angle for descending passes (mean on the left and density on the right) 13

Figure 11 – SAR – PLRM Range difference (m) binned per PLRM SWH and Radial Velocity for ascending passes (mean on the left and density on the right) 14

Figure 12 – SAR – PLRM Range difference (m) binned per PLRM SWH and Radial Velocity for descending passes (mean on the left and density on the right) 14

Figure 13: SWH differences (upper panel) and PLRM SWH (bottom panel) for ascending passes 16

Figure 14: SWH differences (upper panel) and PLRM SWH (bottom panel) for descending passes17

Figure 8 – SWH difference binned per PLRM SWH for ascending (red) and descending (blue) passes 18

Figure 15 – Sigma0 differences (dB) for ascending passes 19

Figure 15 – Roll Angle (degree) for ascending passes 19

Figure 15 – Pitch Angle (degree) for ascending passes 20

Figure 15 – Sigma0 differences (dB) for descending passes 21

Figure 15 – Roll Angle (degree) for descending passes 21

Figure 15 – Pitch Angle (degree) for descending passes 22

Reference documents

RD 1 Boy and Moreau, 2013: F. Boy and T. Moreau, "Algorithm Theoretical Basis Document (ATBD) of the CPP RDSAR numerical retracker for oceans", CNES report, **S3A-NT-SRAL-00098-CNES**

RD 2 Moreau et al., 2013: T. Moreau, F.Boy and M. Raynal, "Product Validation Report (PVR) of the CPP RDSAR numerical retracker for oceans", **CLS-DOS-NT-13-155, WP4000 CP4O**

RD 3 Boy and Moreau, 2013: F. Boy and T. Moreau, "Algorithm Theoretical Basis Document (ATBD) of the CPP SAR numerical retracker for oceans", CNES report, **S3A-NT-SRAL-00099-CNES**

RD 4 Moreau et al., 2013: T. Moreau, F.Boy and M. Raynal, "Product Validation Report (PVR) of the CPP SAR numerical retracker for oceans", **CLS-DOS-NT-13-156, WP4000 CP4O report**

RD 5 Dibarboure, F. Boy, J. D. Desjonqueres, S. Labroue, Y. Lasne, N. Picot, J. C. Poisson, P. Thibaut. Investigating Short-Wavelength Correlated Errors on Low-Resolution Mode Altimetry, Journal of Atmospheric and Oceanic Technology, Volume 31, Issue 6 (June 2014) pp. 1337-1362, doi: http://dx.doi.org/10.1175/JTECH-D-13-00081.1

RD 6 Labroue S., M. Raynal, T. Moreau "Validation report WP 5000 Assessment of CPP PLRM retracking", **CLS-DOS-NT-14-114, WP5000 CP4O**

RD 7 Ollivier et al., 2013: A. Ollivier, M. Guibbaud and S. Labroue, "IOP/GOP ESA Product Validation Report", **CLS-DOS-NT-13-286**

List of Contents

1. Introduction 1
1.1. Purpose and scope 1
1.2. Document structure 1
2. Data and method overview 2
2.1. Data coverage and period 2
2.2. Method description 3
2.2.1. SAR CPP retracking 3
2.2.2. PLRM CPP retracking 3
2.2.3. Edited data 3
3. Validation results and overall assessment 4
3.1. Stand alone assessment of CPP SAR processing 4
3.2. Analysis of long wavelength errors by comparing with PLRM 8
3.2.1. Range errors 8
3.2.2. SWH errors 15
3.2.3. Sigma0 errors 18
4. Conclusions 23

1. Introduction

1.1. Purpose and scope

This document aims at analysing the CPP (CNES Processing Prototype) SAR retracking developed by CNES for the CryoSat-2 mission. A set of dedicated diagnoses has been used to evaluate the quality of this retracking and see if it may improve the sea-level anomaly calculation.

The description and the analysis of all the differences that are reported herein were discussed in a strong scientific collaboration with the algorithm expert/responsible who provides a very useful support to assess the performances of their model, help to identify any unexpected behaviours and finally validate the content of this report.

1.2. Document structure

This document is structured into an introductory chapter followed by three chapters describing:

- the data used and coverage,
- the analysis of the results from the different diagnoses that are used to establish their performance (quantifying their skills and drawbacks), and
- a discussion about these results (section 4).

2. Data and method overview

2.1. Data coverage and period

Two months of CryoSat-2 sea level anomalies (SLA) have been computed at 20 Hz and 1 Hz over all the SAR areas acquired in SAR mode. Two different periods (July 2012 and January 2013) were chosen for the WP5000 with the following rationale:

- The large SAR box over the equatorial Pacific is a site chosen =fro calibrating the retracking algorithm because it provides standard sea state conditions (waves close to 2 m) with only few situations of bloom and rain, with low oceanic variability. The two moths chosen for validation encompass this area.
- The month of July represents quite low sea states in the North hemisphere (Figure 1) while the month of January provides stronger wave values that help to cover a larger range of SWH conditions (Figure 2).

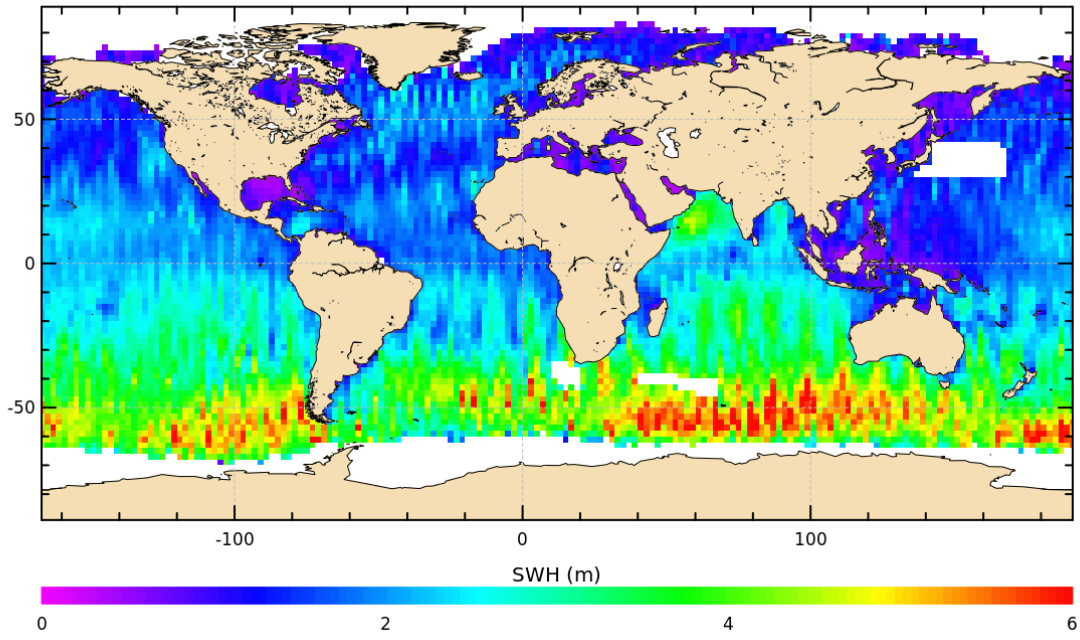

Figure 1: SWH map in July 2012.

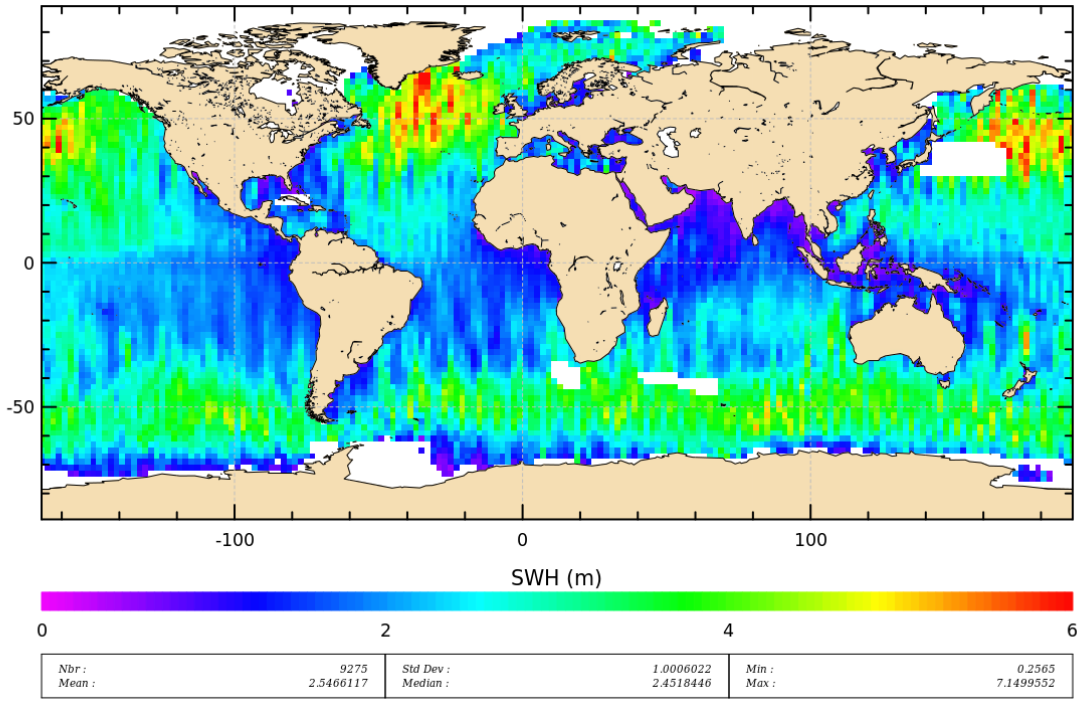

Figure 2: SWH map in January 2013

2.2. Method description

2.2.1. SAR CPP retracking

The method for the CPP SAR retracking is fully described in RD 3 and validation results were already delivered in RD 4.

2.2.2. PLRM CPP retracking

The method for the CPP SAR retracking is fully described in RD 1 and validation results were already delivered in RD 4.

Compared to the results obtained at that time, pLRM data sets have been improved by adding the Look Up Table (LUT) corrections for epoch and SWH that take into account modelling of the PTR and the larger speckle present on PLRM waveforms.

2.2.3. Edited data

Data editing is necessary to remove altimeter measurements having lower accuracy. To analyze the consistency between both wet troposphere solutions in open ocean, only valid ocean data are selected (removing data corrupted by sea ice and rain). Specific editing criteria are applied, based on thresholds on different parameters.

3. Validation results and overall assessment

The validation of SAR processing with Cryosat-2 mission is not straightforward because the SAR mode is activated only over a few areas of the ocean. Therefore, we do not have a complete coverage of the different ocean regimes, neither of the sea states (even if it has been maximised with the two months analysed).

This validation exercise aims at answering the two following questions:

1. Does SAR processing present any long wavelength error compared to LRM processing which has been used for operational oceanography for more than 20 years?
2. The SAR technique should improve the capability of observing small scale content (between 20 km and 100 km) because of the reduced 20 Hz noise coupled with the true resolution of 300 m in the along track direction. Does the SAR help to better retrieve short scale oceanic structures?

For this purpose, the validation is performed with two different approaches. On one hand, we perform stand alone assessment using SAR data only, to assess the performances as it could be done for LRM mode. On the other hand, we use the PLRM measurements that are perfectly collocated and time tagged with the SAR data. We first checked that the PLRM do not present any additional error compared to LRM processing (DR TBD). Such a comparison between SAR and PLRM allows detecting very small errors because the oceanic signal is properly removed, compared to a cross calibration exercise with another mission that needs long time series. This approach helps to make a deep assessment with only two months of data and detecting residual dependence on the order of the centimetre.

We detail the following diagnoses:

- Analysis of spectral content of the different parameters estimated from the waveforms
- Assessment of the large scale biases compared to PLRM data.
- Assessment of residual errors linked to key parameters for the SAR processing

3.1. Stand alone assessment of CPP SAR processing

The three parameters retrieved by the retracking are analysed here focusing on the spectral content of the Sea Level Anomaly (Figure 3), SWH (Figure 4) and sigma0 (Figure 5). The plots have been computed over the 2 months of data, merging all the SAR areas, except for the SLA for which we have focused on the Pacific area. The PSD obtained for PLRM parameters are also plotted for comparison.

As expected, the SAR 20 Hz noise is smaller than PLRM noise with 5.7 cm and 11.3 cm respectively. Note that this value corresponds to the noise for the mean SWH over the Pacific and the 2 months considered. It is not the 20 Hz noise at 2m waves which is usually given in altimeter error budget.

The other important feature is that the SAR PSD does not show the energy plateau between 10 and 30 km that we observe on the PLRM (referred as a “bump” error). This error was studied in Dibarboure et al 2014 and found to affect all the altimeters in LRM mode. The cleaner PSD of SAR SLA should yield more accurate observations of the SLA at small scales.

Furthermore, the SAR PSD shows that the SAR processing also improves the content at larger scales above 100 km, with the SAR PSD showing less energy between 100 and 250 km. In this case, we see that the bump energy coupled with the 20 Hz noise of the PLRM alters the oceanic slope for scales up to 250 km. The oceanic slope derived with the SAR data is steeper and corrects the error made on the slope derived from LRM data due to the bump error.

The PSD for LRM SWH also shows the bump error whereas the SAR curve shows a more continuous decay. The 20 Hz noise for SAR SWH is close to 40 cm which is below the 20 Hz noise observed on Jason-2 SWH (average value is close to 54 cm), but not as low as expected by the theory.

The PSD for sigma0 show very similar curves. The only discrepancy is found for scales between 16 and 60 km, but also between 2.5 and 7 km where the SAR sigma0 has more energy. This is explained by the smoothing of the sigma0 done in LRM processing due to the size of the footprint. The SAR with the 300 m resolution is able to capture small scale variations of the sea surface roughness thus providing more energy, whereas the LRM measurement smoothes all these variations. This increase of energy corresponds to the scales where the bump error is present on PLRM SLA PSD. We believe that the SAR processing better captures the sea surface roughness in the sigma0, thus providing a cleaner SLA observation.

Figure 6 shows an example of sigma0 variations observed with PLRM and SAR processing in a case of a very calm sea. The SAR sigma0 exhibits small scales structures of 10-30 km size that are smoothed by the PLRM sigma0. The curves of the 20 Hz SLA observed on the same segment show that the SAR profile remains very stable compared to PLRM data. The stronger case is located between 42° and 42.1°, but we also observe some smaller jumps in the PLRM SLA (41.6° and 42.4°). Focusing on the 20 km between 41.9° and 42.1°, there is a perfect correlation between the SAR sigma0 and the PLRM SLA that departs from the mean signal by +/- 30 cm. This example shows that the SAR and PLRM behave differently in case of heterogeneity of the surface. With PLRM processing, the signal is seen on the SLA and the sigma0 remains stable whereas all the roughness is properly retrieved along track by the SAR sigma0 and does not corrupt the SLA measurement. Nevertheless, the SAR SLA is also affected in some cases, which would suggest that the SAR processing could be further improved.

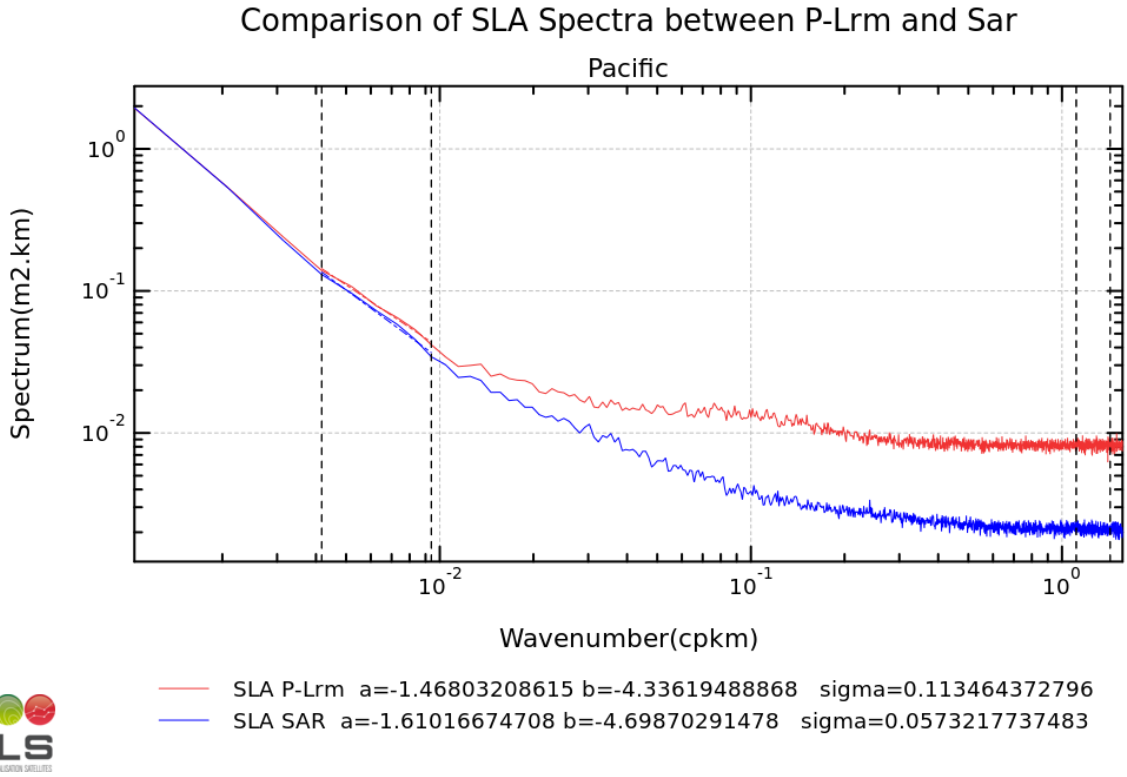

Figure 3: PSD of SAR and LRM SLA

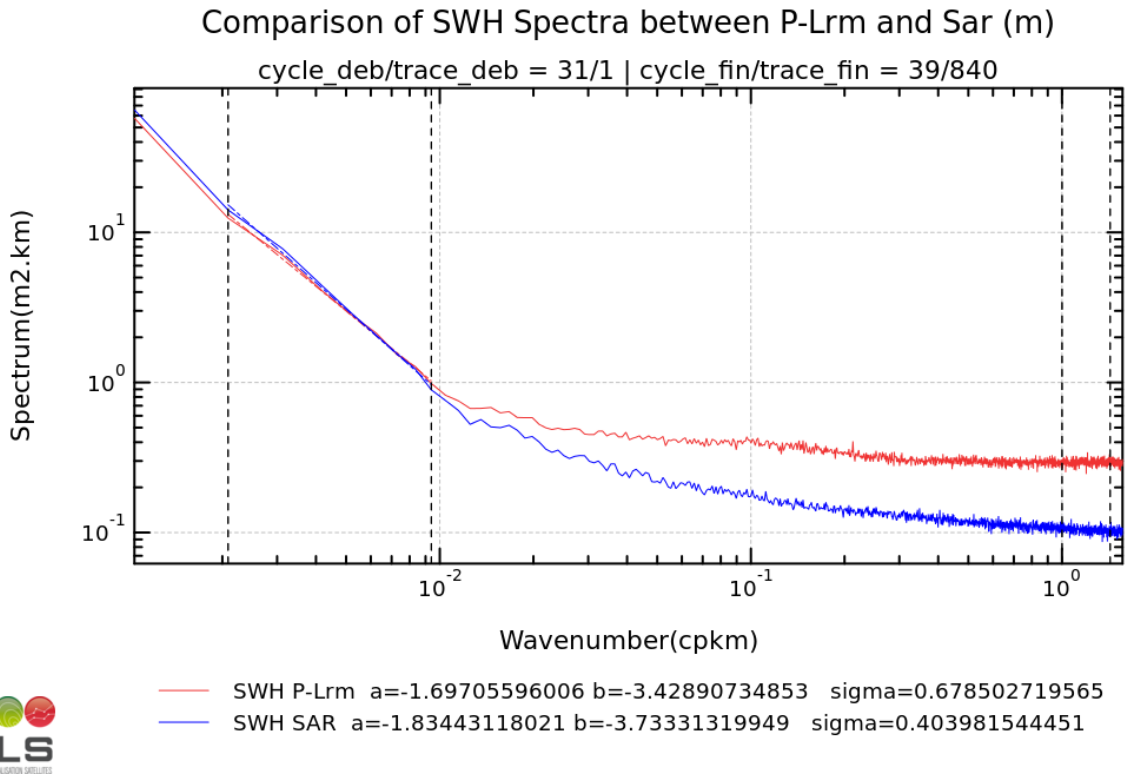

Figure 4: PSD of SAR and LRM SWH

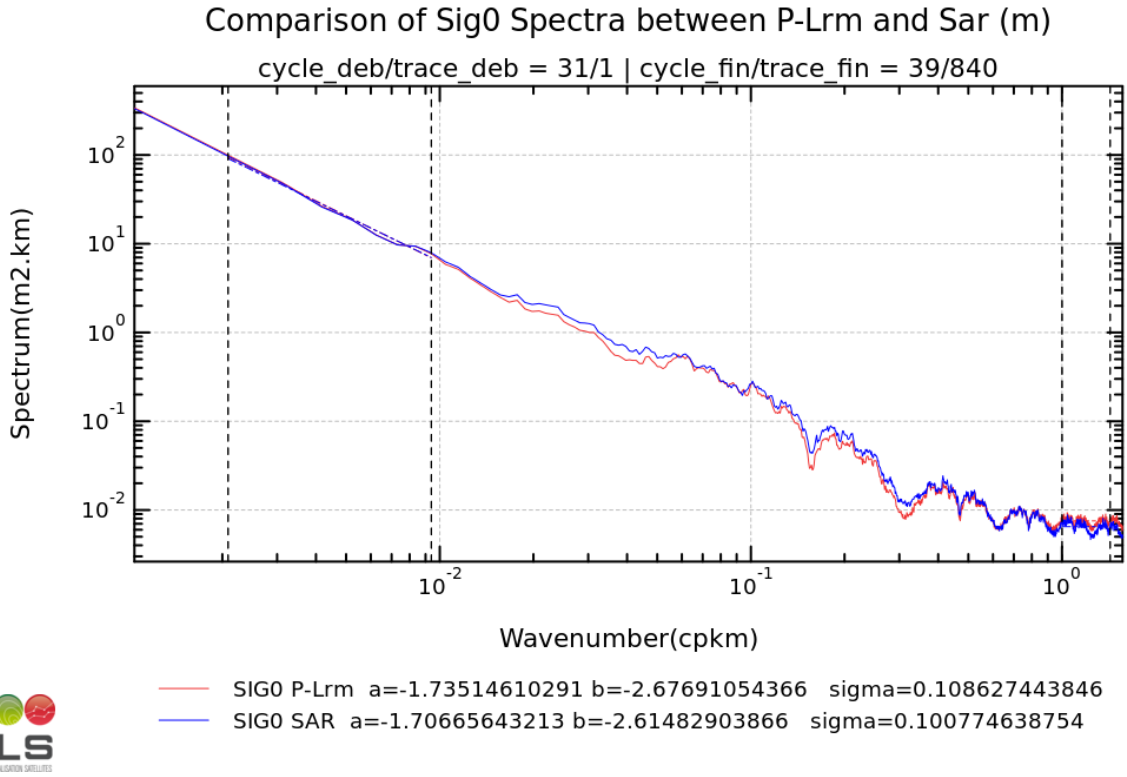

Figure 5: PSD of SAR and LRM Sigma0

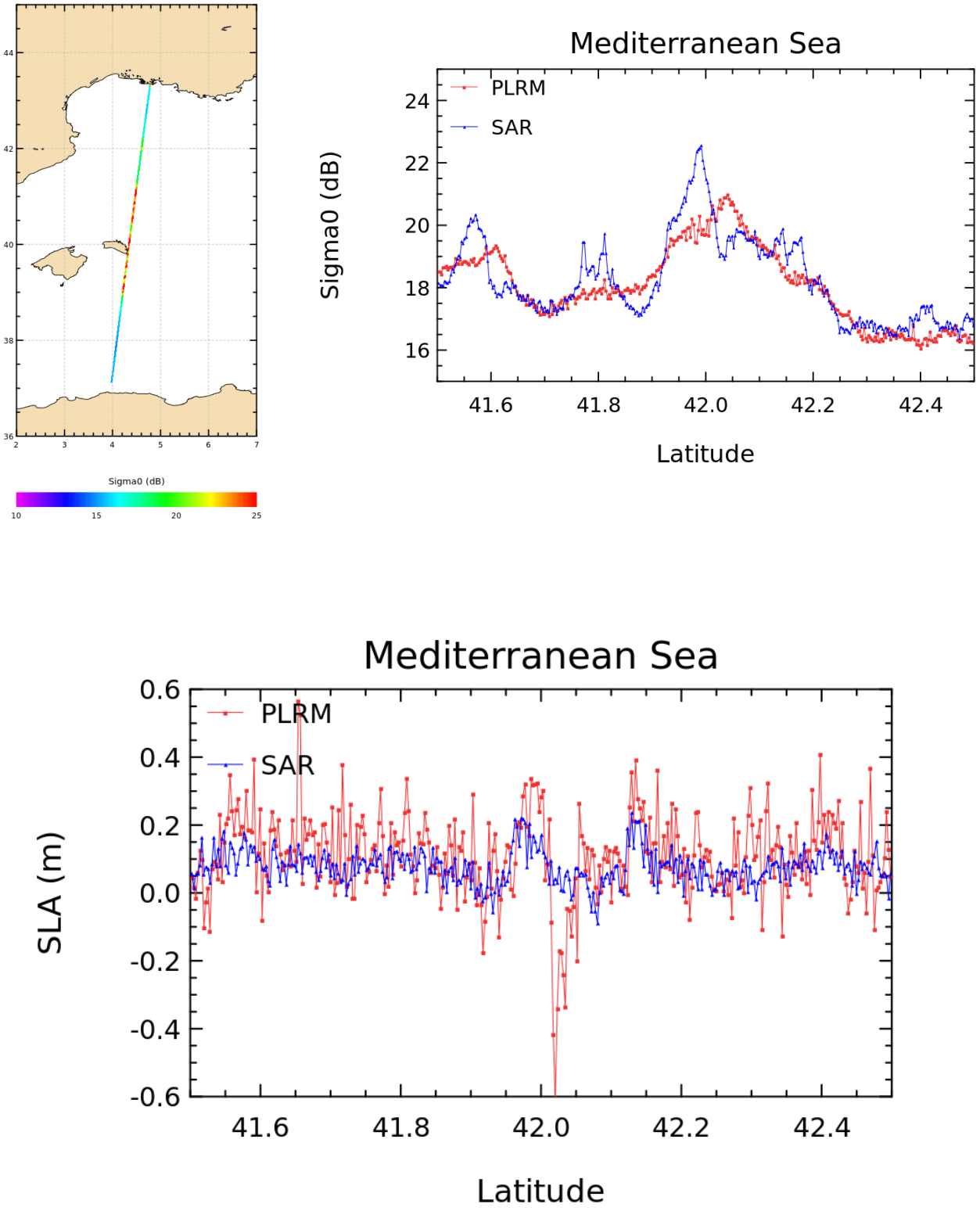

Figure 6 – Sigma0 for PLRM (red) and SAR (blue) and for Sea Level Anomaly for PLRM (red) and SAR (blue). The map of the SAR sigma0 is shown on the left upper panel.

3.2. Analysis of long wavelength errors by comparing with PLRM

3.2.1. Range errors

The maps of the difference between SAR and PLRM SLA are given in Figure 7 and Figure 8 for ascending and descending passes respectively. Both maps exhibit an excellent agreement between both processings, showing variations of only 2 cm magnitude! Several features already come out from this simple comparison:

- The geographic pattern of 2 cm magnitude is correlated with the waves, with higher differences encountered for stronger waves. It could be either an error in the SAR retracking or a different behaviour of the SSB between SAR and PLRM processings.
- The maps do not clearly show residual errors correlated with other parameters such as roll angle or radial velocity.
- The absolute constant bias between SAR and PLRM is found in areas that present very low sea sates such as the Mediterranean basin and Black sea. This means that we observe a mean bias of 3 cm, SAR range being too long.

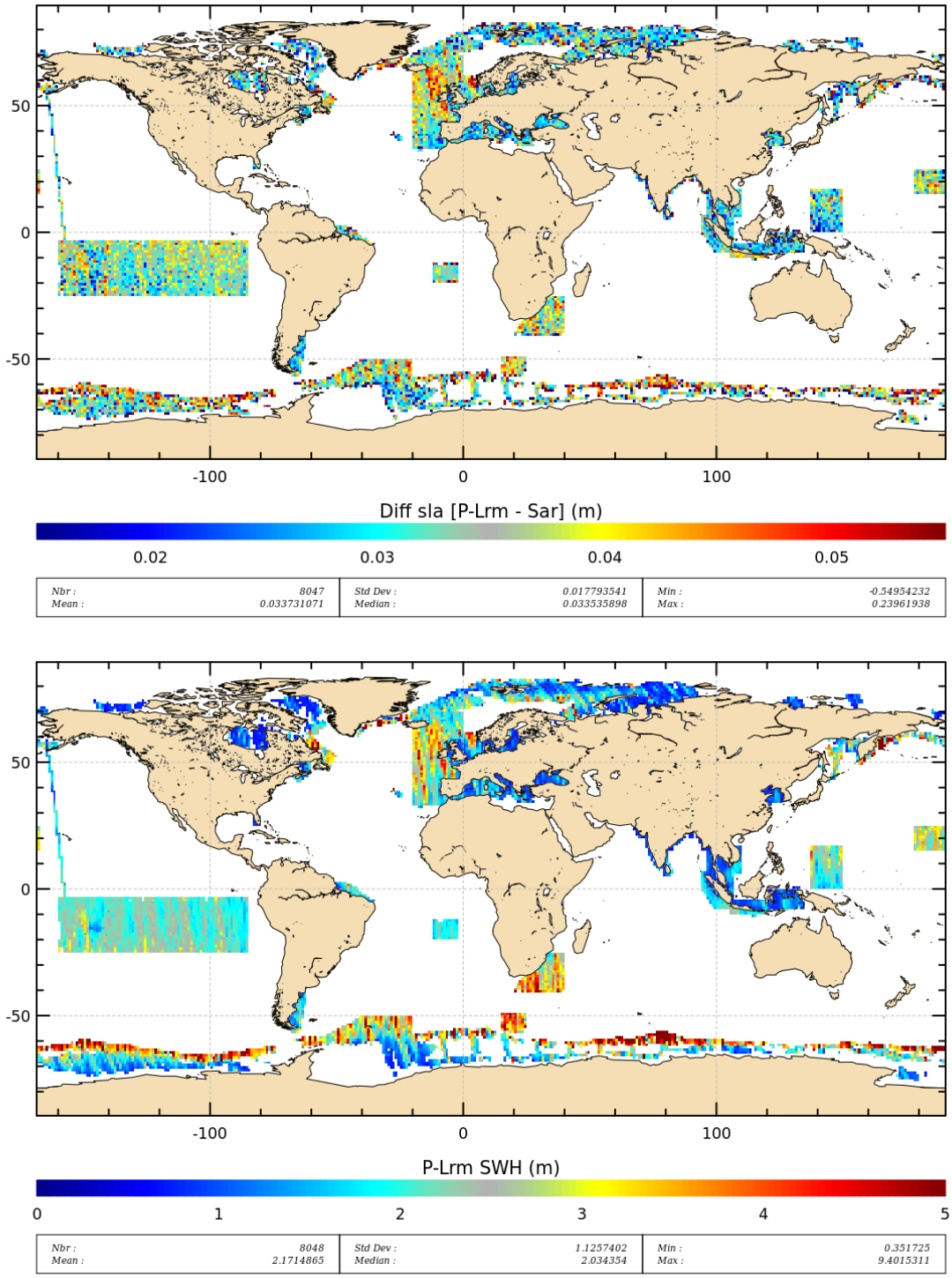

Figure 7: SLA differences (upper panel) and PLRM SWH (bottom panel) for ascending passes

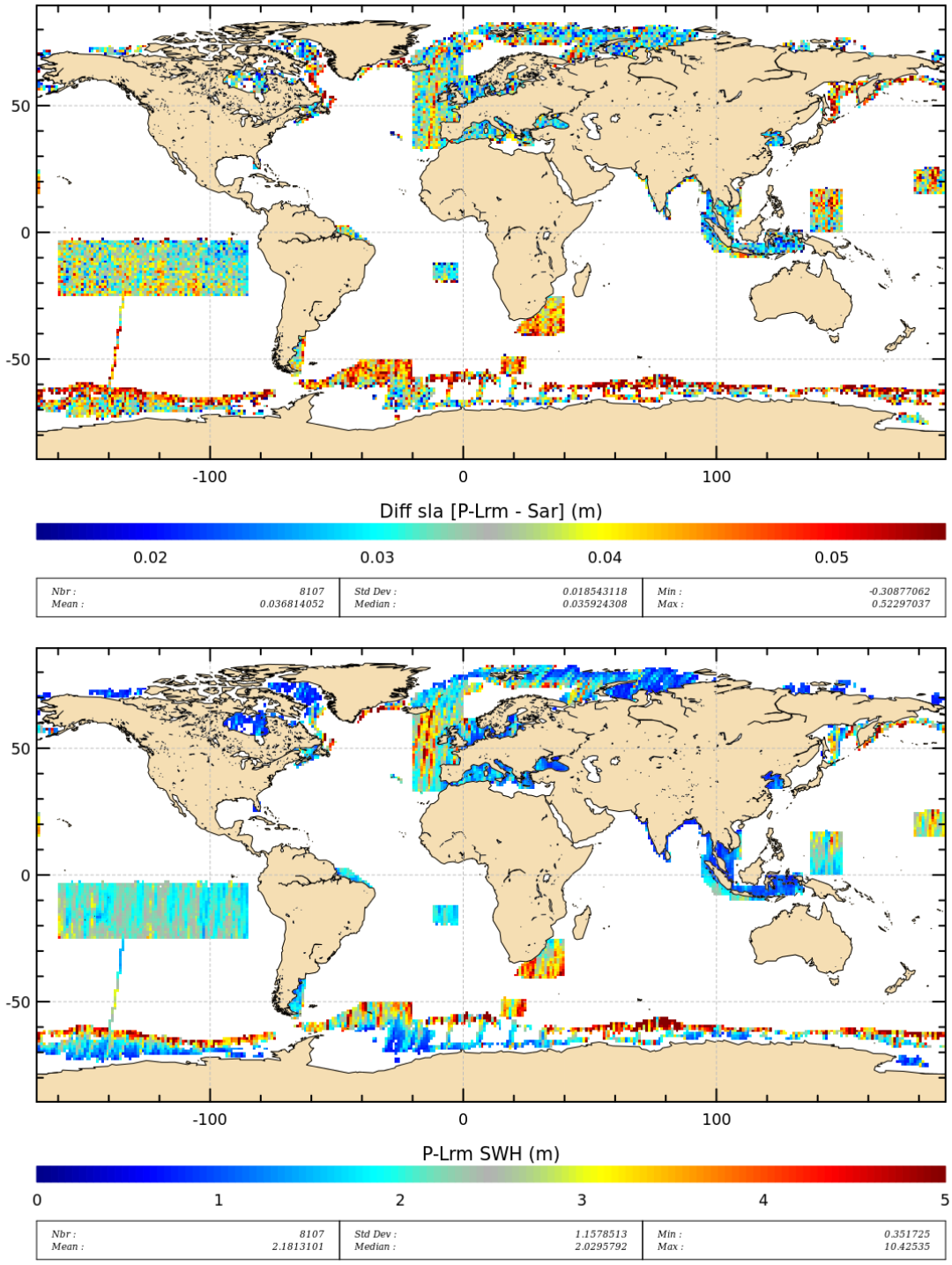

Figure 8: SLA differences (upper panel) and PLRM SWH (bottom panel) for descending passes

Figure 9 focuses on the signal correlated with the waves. All range differences are averaged per bin of PLRM SWH taken as a reference. The dependence with respect to waves is the same for ascending and descending passes, close to 0.4% SWH. This result suggests that the CPP SAR data would present a Sea State Bias different from the LRM mode by 0.4%SWH. The CPP SAR would yield a higher SSB compared to LRM mode.

The two curves show a mean constant bias between ascending and descending differences of 4 mm. We cannot conclude if this difference comes either from the PLRM or the SAR or both of them.

This plot also confirms that the absolute bias between SAR and PLRM is close to +3 cm as already observed on the maps, but with different values for ascending and descending passes (roughly 2.8 cm for ascending and 3.2 cm for descending). Note that the absolute bias is given by the value of the range difference at very low sea states rather than taking the mean value of the difference (close to 2.7 m of waves in general) which contains the absolute bias and the SSB difference between both data sets.

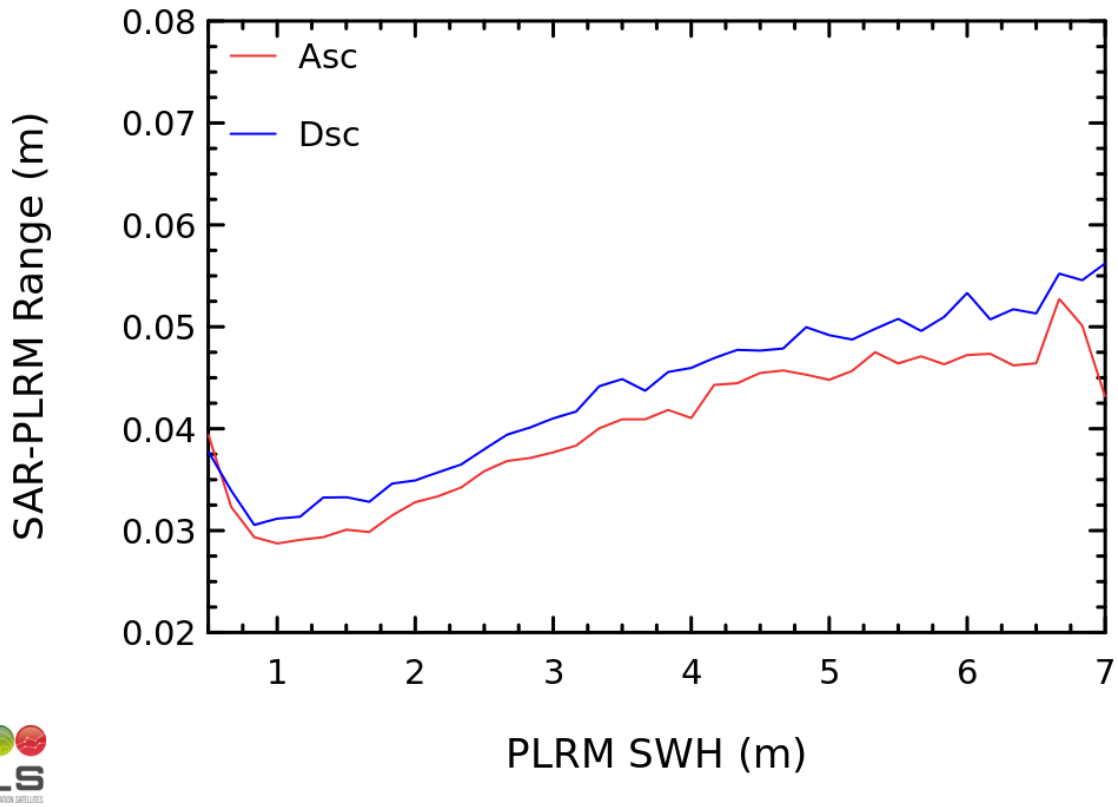

Figure 9 – Range difference binned per PLRM SWH for ascending (red) and descending (blue) passes

The sensitivity to other key parameters is also analysed. We mainly focus on popssible correlation with mispointing (especially with the roll angle) and with radial velocity because these are parameters that can induce errors in SAR retracking.

Figure 10 and Figure 11 show the range differences binned per PLRM SWH and roll angle values. This king of diagnosis with two correlatives better separate the correlations between the different parameters. For the ascending passes, we have a roll angle distribution that presents very small range scale and prevents from checking dependency with the roll angle. But the descending passes exhibit values between -0.08 and - 0.18 degree that help to check that there are no variations wrt roll angle. We can only see the correlation with SWH that dominates the plot.

In the same way, Figure 12 and Figure 13 show the correlation with PLRM SWH and radial velocity separating ascending and descending passes. There is no clear dependency wrt to radial velocity. This analysis should be completed with more data in order to get more wave situations associated to different radial velocities.

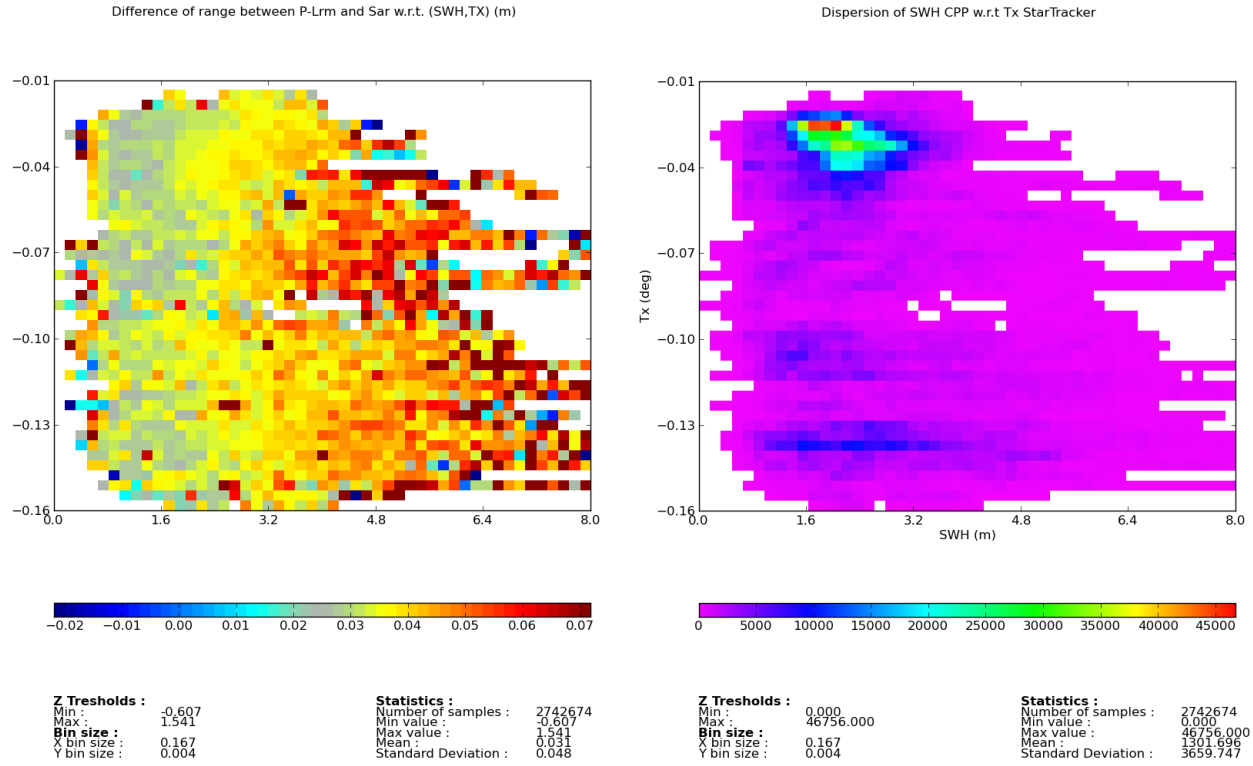

Figure 10 – SAR – PLRM Range difference (m) binned per PLRM SWH and Roll Angle for ascending passes (mean on the left and density on the right)

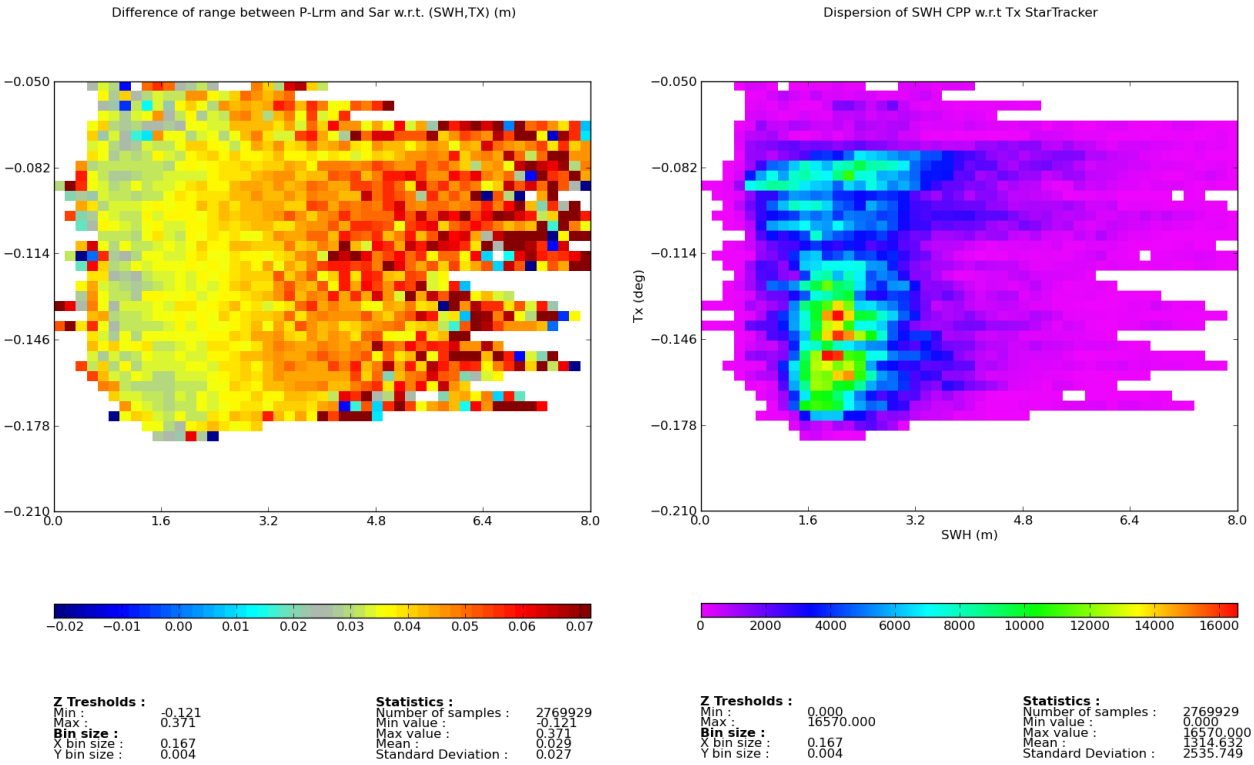

Figure 11 – SAR – PLRM Range difference (m) binned per PLRM SWH and Roll Angle for descending passes (mean on the left and density on the right)

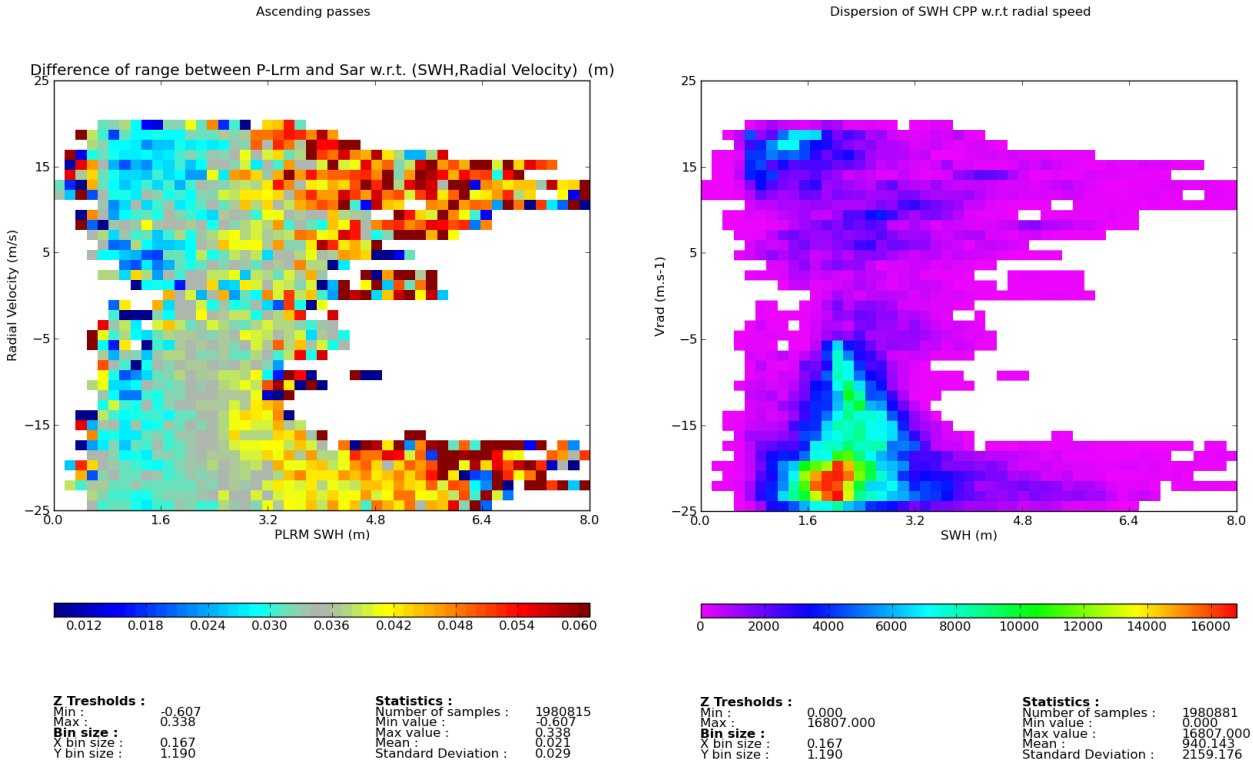

Z Tresholds : Min : -0.607 Max : 0.338 **Bin size :** X bin size : 0.167 Y bin size : 1.190

Statistics : Number of samples : 1980815 Min value : -0.607 Max value : 0.338 Mean : 0.021 Standard Deviation : 0.029

Z Tresholds : Min : 0.000 Max : 16807.000 **Bin size :** X bin size : 0.167 Y bin size : 1.190

Statistics : Number of samples : 1980881 Min value : 0.000 Max value : 16807.000 Mean : 940.143 Standard Deviation : 2159.176

Figure 12 – SAR – PLRM Range difference (m) binned per PLRM SWH and Radial Velocity for ascending passes (mean on the left and density on the right)

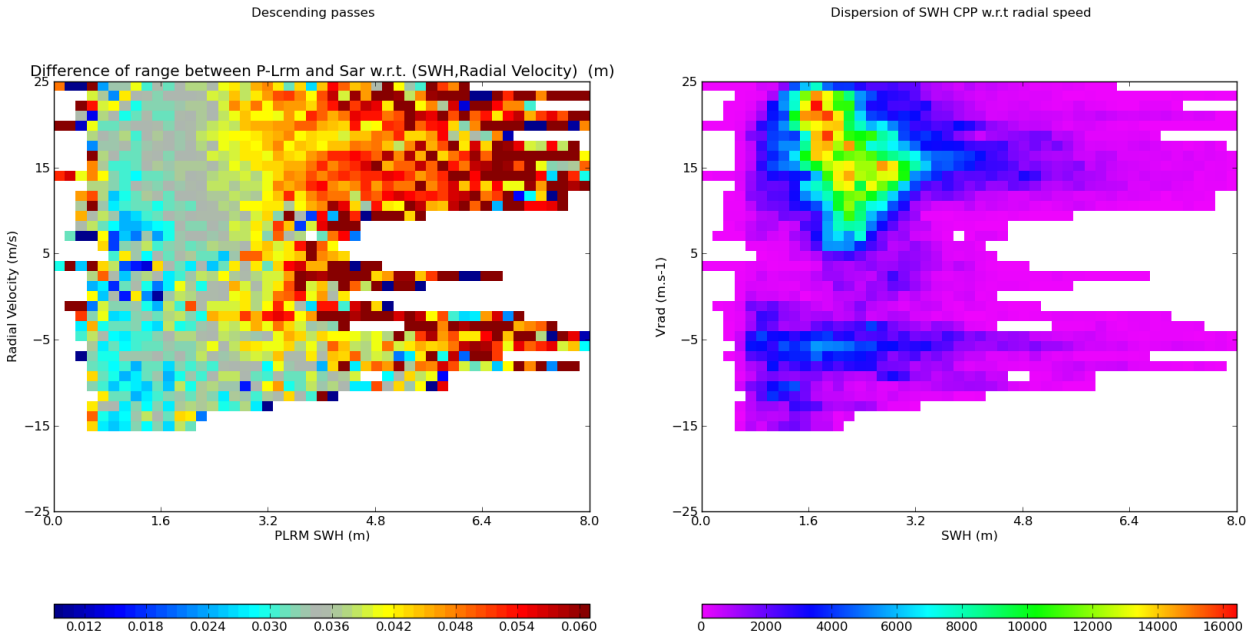

Z Tresholds : Min : -0.086 Max : 0.653 **Bin size :** X bin size : 0.167 Y bin size : 1.190

Statistics : Number of samples : 2442988 Min value : -0.086 Max value : 0.653 Mean : 0.026 Standard Deviation : 0.031

Z Tresholds : Min : 0.000 Max : 16416.000 **Bin size :** X bin size : 0.167 Y bin size : 1.190

Statistics : Number of samples : 2442988 Min value : 0.000 Max value : 16416.000 Mean : 1159.463 Standard Deviation : 2549.126

Figure 13 – SAR – PLRM Range difference (m) binned per PLRM SWH and Radial Velocity for descending passes (mean on the left and density on the right)

3.2.2. SWH errors

The difference between SAR and PLRM SWH are given in Figure 14 and Figure 15 for ascending and descending passes respectively. Both maps show a clear correlation with the waves with a difference close to -10 cm for very low waves (in the Mediterranean Sea and Black Sea) and up to +25 cm for stronger waves. Note that the PLRM waves have been assessed in RD 6 and found to be too low by 10 cm over the Pacific area with respect to Jason-2 waves. This implies that the SAR waves are only 5 cm too high over the Pacific area (ranges are comprised between 1 and 3 m).

Figure 16 shows the SWH difference plotted as a function of the PLRM SWH. Assuming a constant bias of -10 cm on the PLRM SWH, this curve shows that the SAR SWH are unbiased for waves close to 1.25 m and there is a linear error depending on the waves (roughly 4% SWH) between 1.25 m and 5 m. The bias seems to saturate at a constant value for stronger waves. The case of the lower waves shows larger errors meaning that the SAR processing tends to under estimate waves below 1 m.

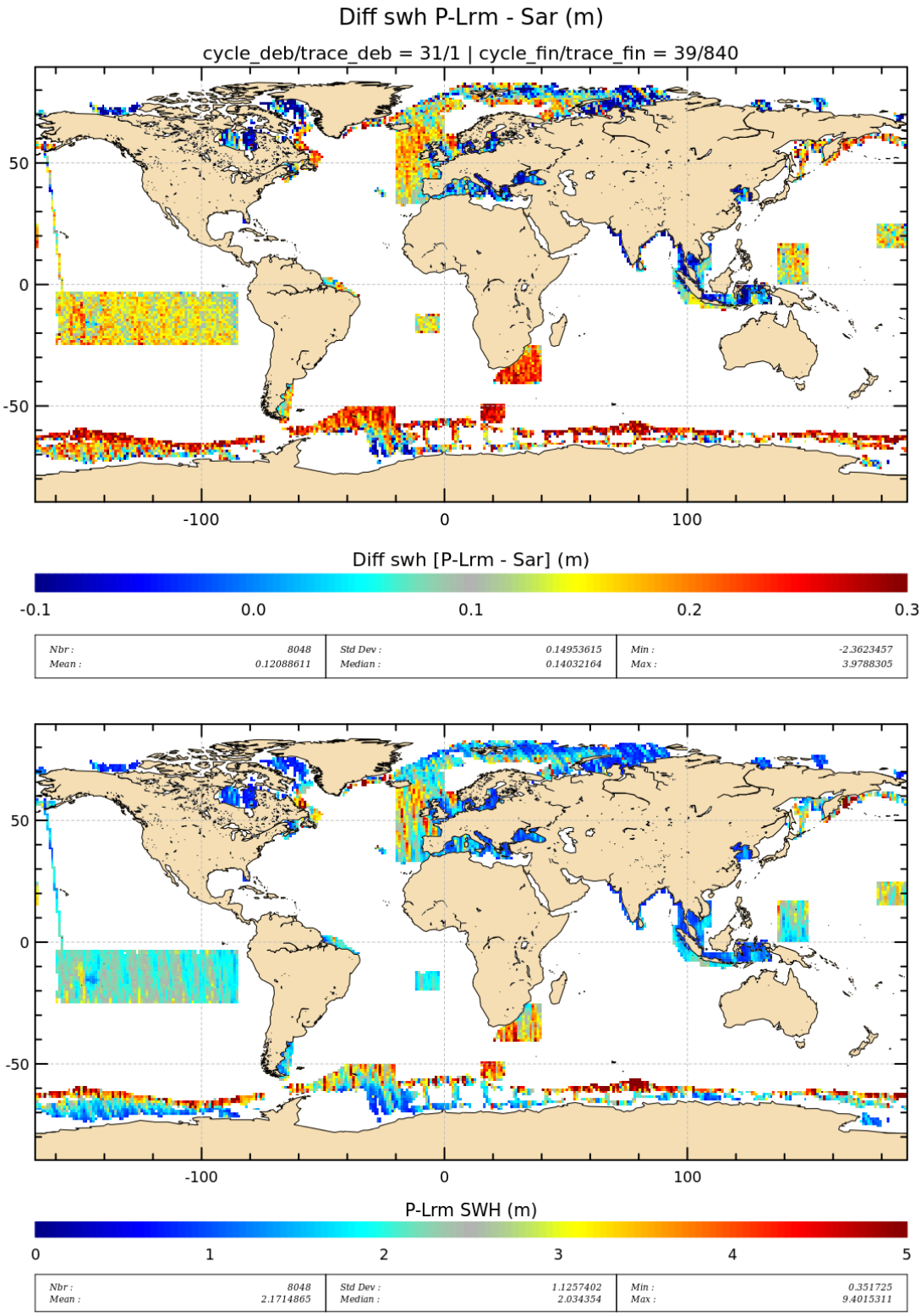

Figure 14: SWH differences (upper panel) and PLRM SWH (bottom panel) for ascending passes

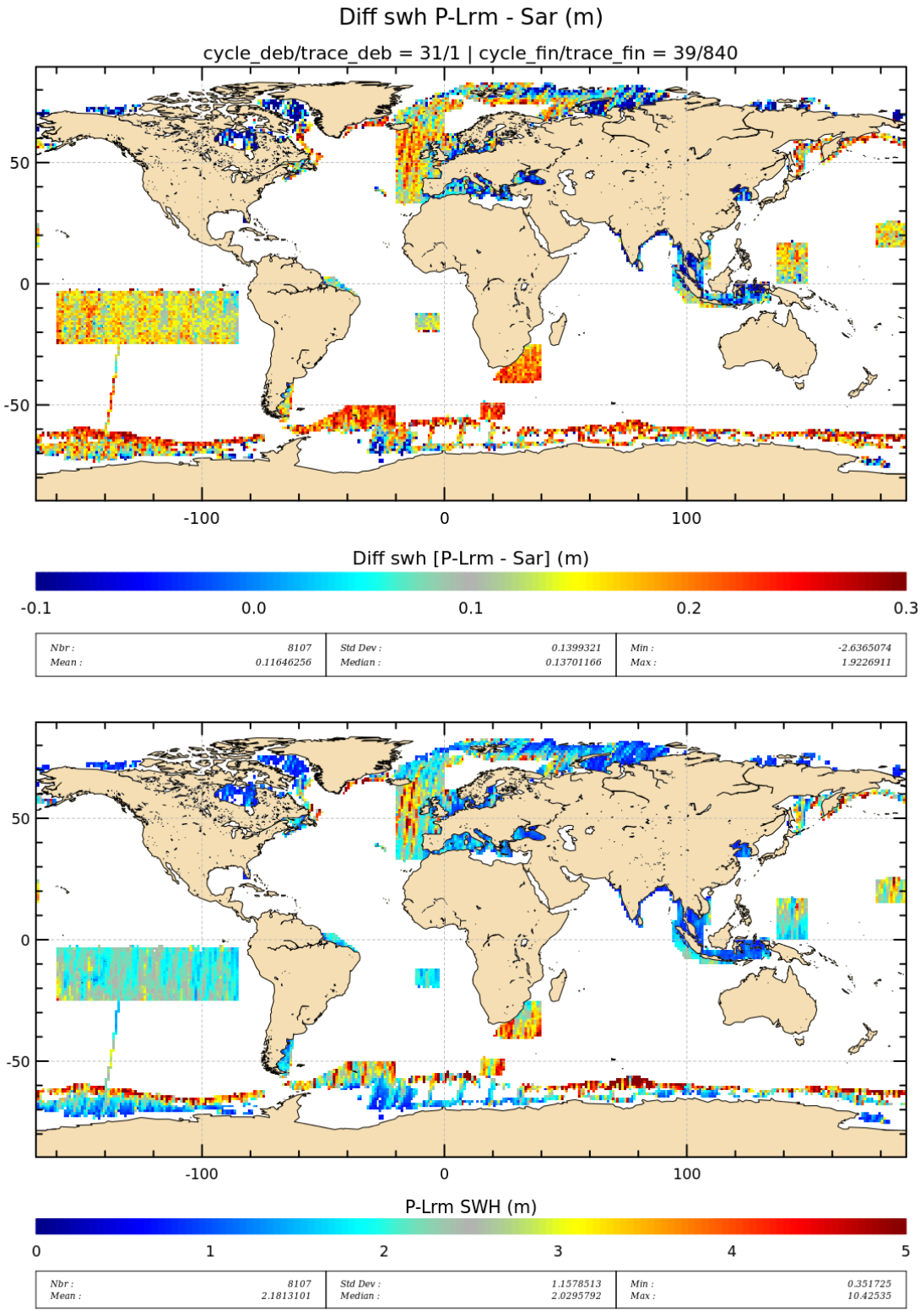

Figure 15: SWH differences (upper panel) and PLRM SWH (bottom panel) for descending passes

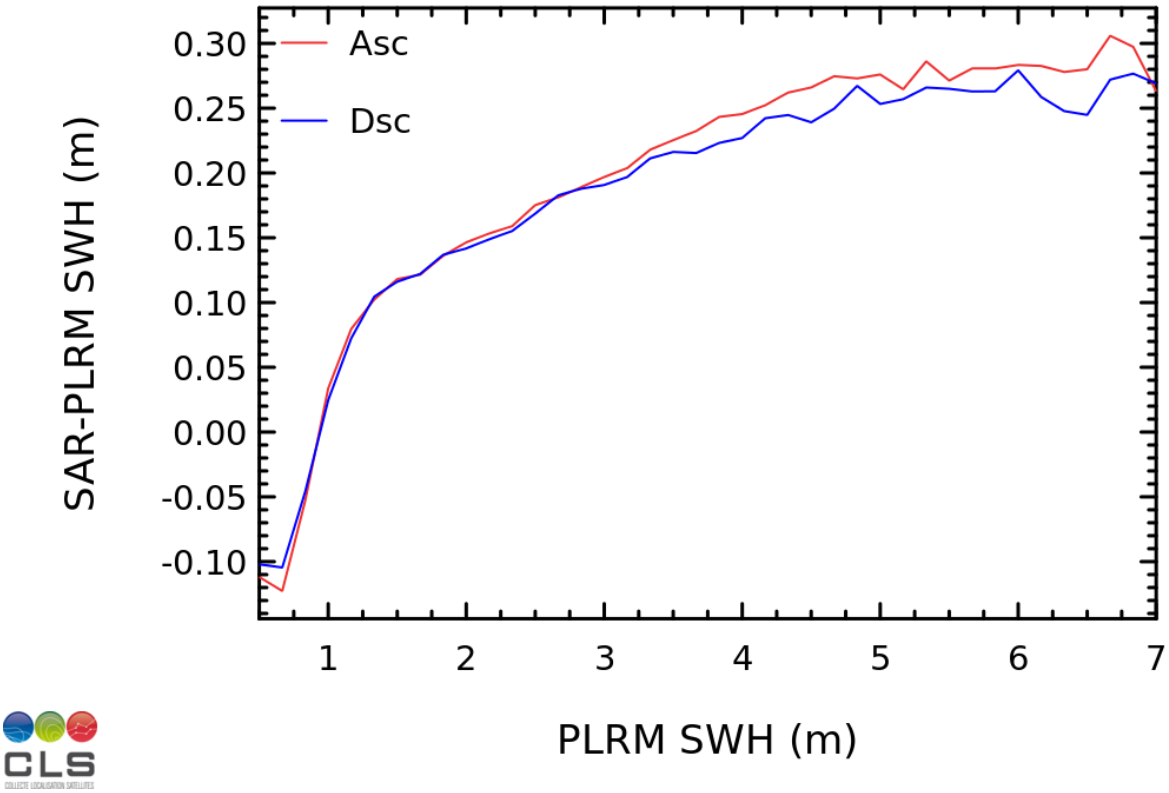

Figure 16 – SWH difference binned per PLRM SWH for ascending (red) and descending (blue) passes

3.2.3. **Sigma0 errors**

Figure 17 and Figure 20 show the difference of sigma for ascending and descending passes respectively. Both maps exhibit a mean bias of 0.4 dB, SAR sigma0 being higher than PLRM sigma0. Note that the PLRM sigma0 has been biased to the Jason-2 mean value but there can still have residual bias of a few tens of dB.

We are more interested in the geographical variations of the difference which are very small. Indeed, we see variations of only 0.2 dB magnitude which show correlations with pitch and roll angles derived form the star tracker information.

The maps of the roll and pitch (Figure 18, Figure 19, Figure 21, Figure 22) show that the patterns on the sigma0 difference are either correlated with roll or pitch angles depending on the areas and the type of tracks. For instance, the descending Pacific is perfectly correlated with the roll but the patterns do not match in all regions: the areas above 50S are not so well correlated with the roll. In the same manner, the correlation with the roll in the Pacific for the ascending passes is less obvious. Even if the ascending map for the roll shows variations, they are not reflected in the map of the ascending sigma0 difference which is quite homogeneous.

We need a longer time serie to further understand if this difference is explained by the pitch or roll taken into account in the SAR processing. We also have to check if such an error of 0.2 dB comes either from the SAR processing or from the PLRM processing.

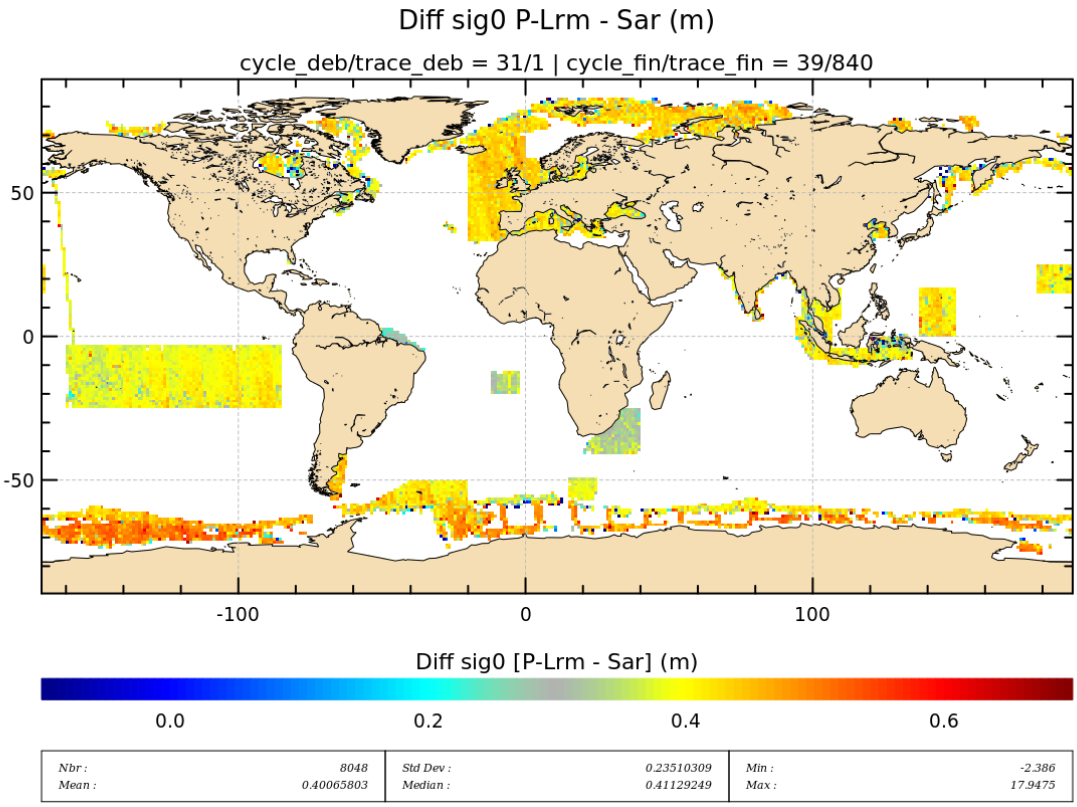

Figure 17 – Sigma0 differences (dB) for ascending passes

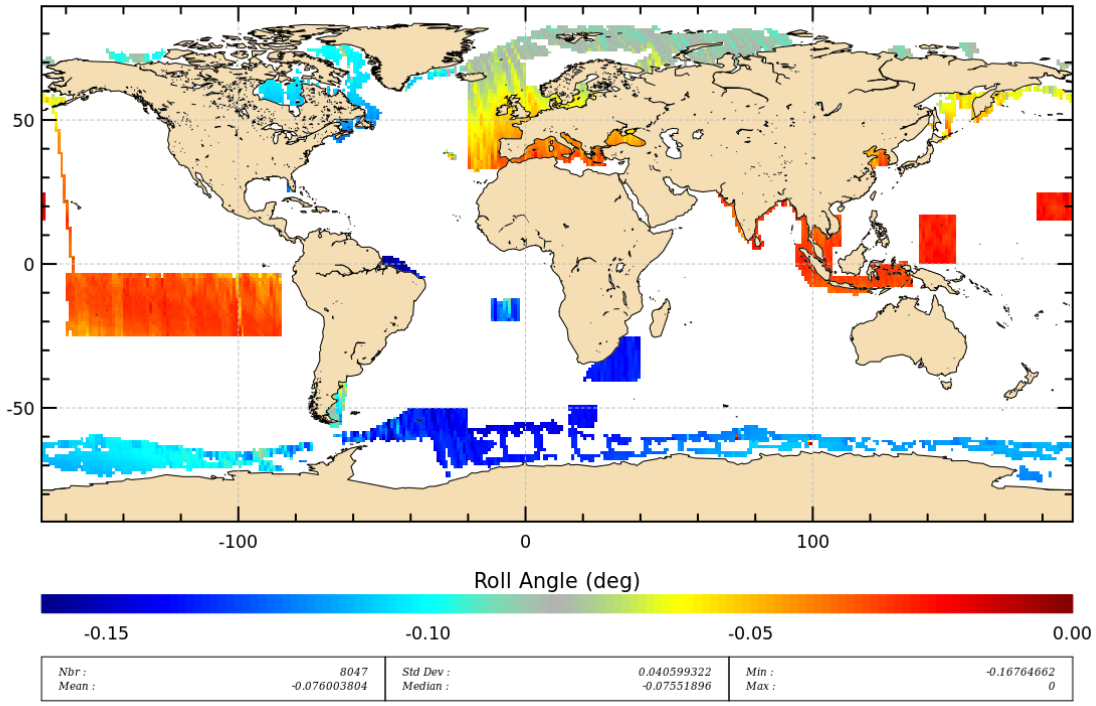

Figure 18 – Roll Angle (degree) for ascending passes

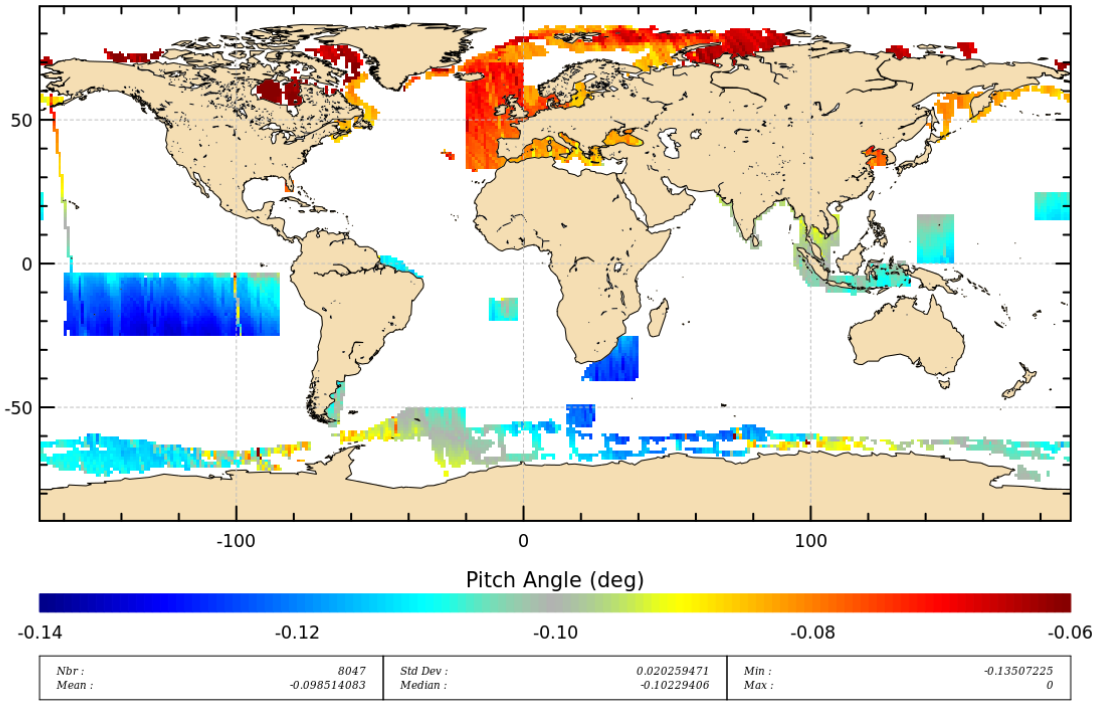

Figure 19 – Pitch Angle (degree) for ascending passes

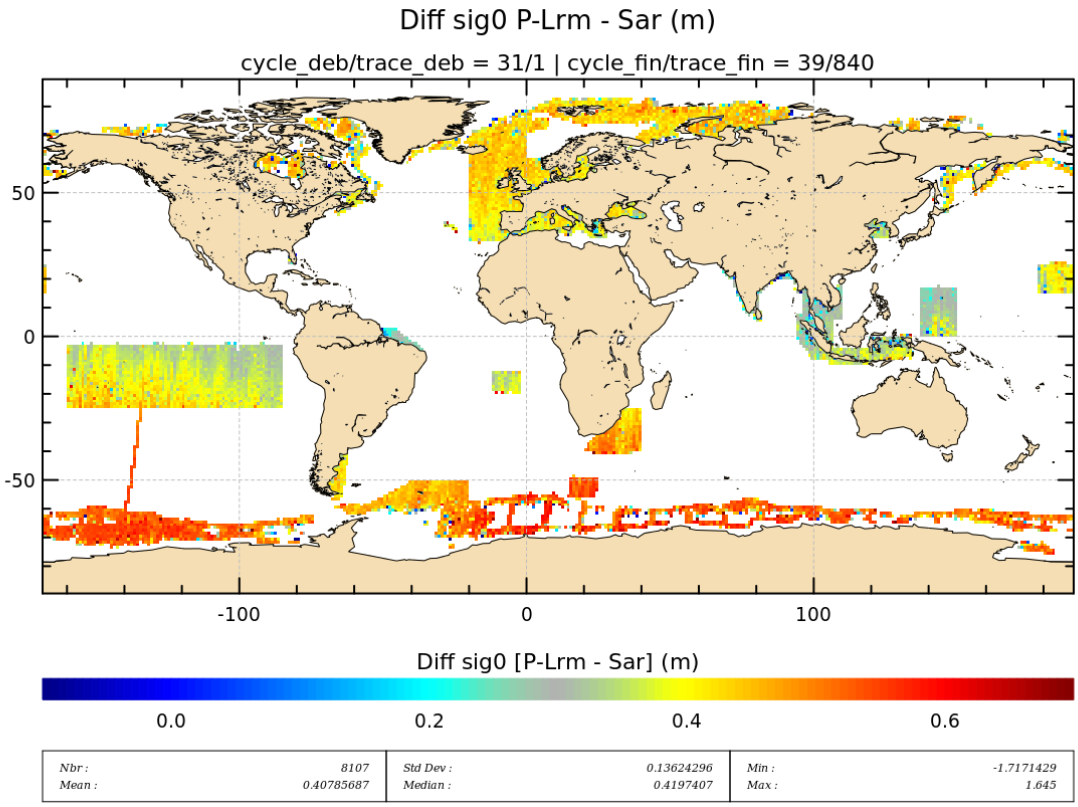

Figure 20 – Sigma0 differences (dB) for descending passes

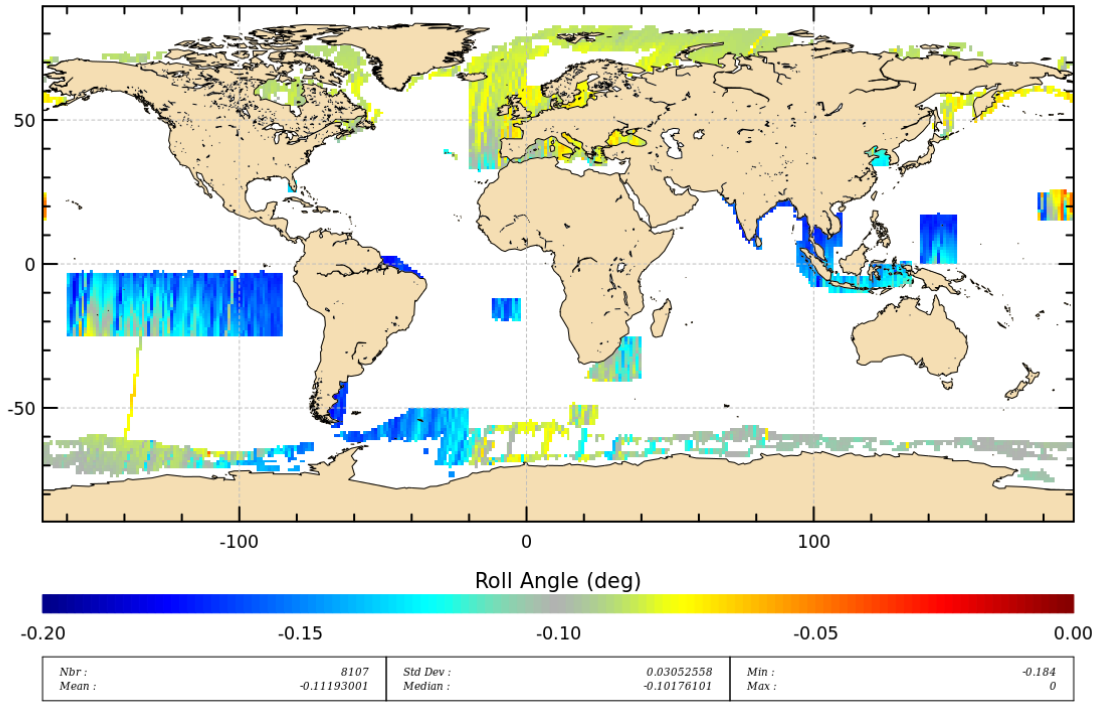

Figure 21 – Roll Angle (degree) for descending passes

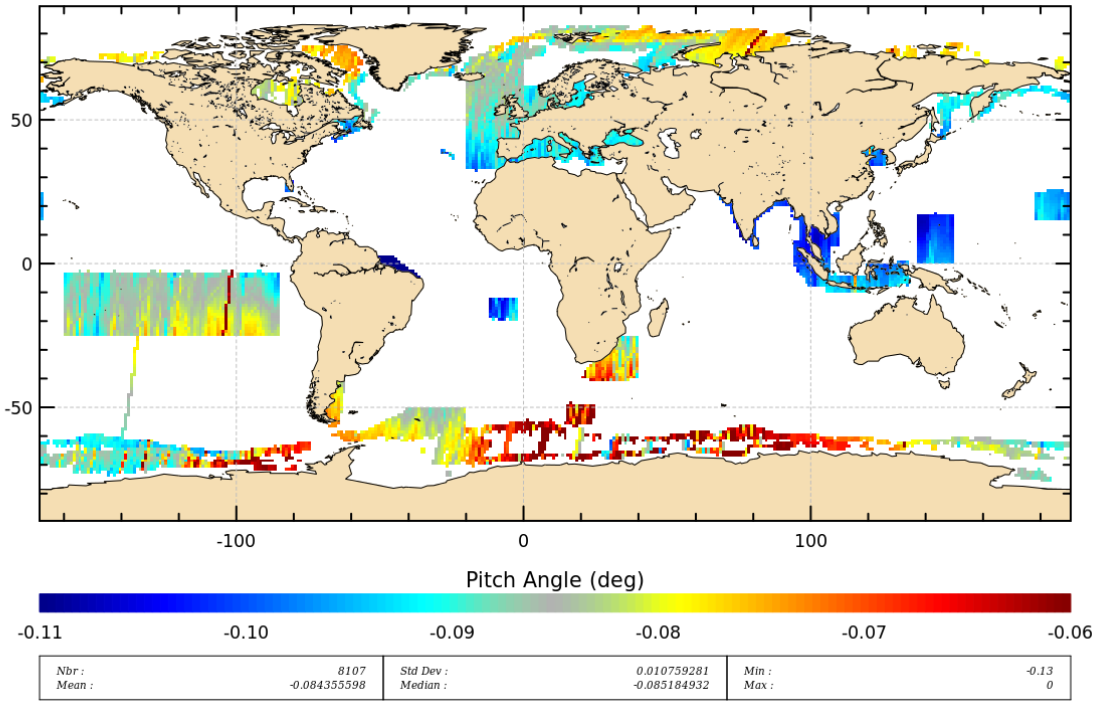

Figure 22 – Pitch Angle (degree) for descending passes

4. Conclusions

The main findings are summarised below:

1. SAR CPP processing shows improved content for SLA, SWH and Sigma0 at scales below 100 km. The more continuous decay of the SLA PSD should yield better observations to capture oceanic structures below 100 km.
2. The Sigma0 provides more short scale content an thus more accurate content due to the 300 m footprint in the along track direction.
3. The SLA show neither residual errors correlated to mispointing, nor to radial velocity. Only long wavelength error correlated with SWH has been found, which would suggest either an error in the SAR retracking or a different SSB behaviour between LRM and SAR modes with the CPP processing. The impact on this data set is close to 0.4% SWH, providing a SAR SSB higher than the LRM SSB. This effect on SSB should be further confirmed with other SAR retrackings.
4. The SWH exhibit residual error correlated with SWH close to 4% SWH.
5. The Sigma0 shows negligible bias of 0.2 dB magnitude, possibly correlated with mispointing.
6. The absolute biases on SAR parameters are close to 3 cm for range, 5 cm for SWH and 0.4 dB for sigma0.